Commun. Theor. Phys. **64** (2015) 735–740 Vol. 64, No. 6, December 1, 2015

Theoretical Analysis of Spectral Correlations Between Photon Pairs Generated in Nanoscale Silicon Waveguides*

LU Liang-Liang (陆亮亮),[1] XU Ping (徐平),[1,†] XU Jian-Ning (徐建宁),[1] HE Guang-Qiang (何广强),[2] and ZHU Shi-Ning (祝世宁)[1]

[1]National Laboratory of Solid State Microstructures and School of Physics, Nanjing University, Nanjing 210093, China
[2]State Key Laboratory of Advanced Optical Communication Systems and Networks, Department of Electronic Engineering, Shanghai Jiaotong University, Shanghai 200240, China

(Received August 20, 2015; revised manuscript received September 9, 2015)

Abstract *Spontaneous four wave mixing in nonlinear waveguide is one of the excellent technique for generating photon pairs in well-defined guided modes. Here we present a comprehensive study of the frequency characteristic of correlated photon pairs generated in telecom C-band from a dispersion-engineered silicon wire waveguide. We have demonstrated that the waveguide configuration, shape of pump pulse, two-photon absorption as well as linear losses have significant influences on the biphoton spectral characteristics and the amount of frequency entanglement generated. The superior performance as well as the structural compactness and CMOS compatibility makes the silicon wire waveguide an ideal integrated platform for the implementation of on-chip quantum technologies.*

PACS numbers: 42.50.Dv, 03.65.Ud, 42.50.Ar
Key words: four-wave mixing, silicon wire waveguide, frequency correlation

1 Introduction

Recent work in quantum information science has produced a revolution in the understanding of quantum entanglement.[1] The phenomenon of quantum entanglement whereby distant systems can manifest perfectly correlated behavior is now recognized as the key ingredient in performing tasks, which can not be completed with classically correlated systems. Photon-pair generation by spontaneous four wave-mixing (SFWM) has been attracting much attention.[2−5] In optical fibers, it was shown that such photon pairs can be efficiently generated in well-defined single fiber modes and conveniently manipulated by linear optical devices.[6−9] However, there is a drawback with fiber-based entanglement sources, namely the burdensome broadband spontaneous Raman scattering (SpRS), which needs to be suppressed by the aid of auxiliary cooling techniques. Recently, Cui *et al.*[7−8] used photonic crystal fiber (PCF) based sources with large frequency detuning between signal and idler photons to get rid of the contamination of Raman scattering as well as bridged visible and telecom wavelengths.

In parallel, SFWM in a nano-scale silicon wire waveguide (SWW) based on silicon-on-insulator (SOI) structure has attracted much attention as a new way to generate entangled photon pairs due to the high intrinsic nonlinearity, the possibility for dense integration, mature fabrication methods, low loss and low manufacturing cost.[10−17] In particular, the deleterious SpRS noises in the SWW can be effectively eliminated because of the crystalline nature of silicon material, which leads to significantly lesser broadening of the Raman vibrational modes. The noise can be further suppressed by selecting signal and idler frequencies that are far from the Raman peak, which is 15.6 THz from the pump frequency and has a narrow bandwidth about 100 GHz.[11−12] Such silicon-based photon sources not only exhibit high pair correlation but also have high spectral brightness.[13] In addition, in the SFWM process, the four photons involved in the nonlinear process have similar frequencies, hence the temporal walkoff between a pump and a photon pair is negligible. The superior performance as well as the structural compactness and CMOS compatibility makes the SWW an ideal integrated platform for the implementation of on-chip quantum technologies.

However, the characteristics of frequency correlation in an SWW have not been studied in detail. Grice *et al.*[18] first studied the elimination of spectral correlations for photon pairs generated from spontaneous parametric down-conversion by the method of group-velocity matching using a broadband pump pulse. Then Garay–Palmett *et al.*[19] extended this method to the case of SFWM by engineering the group velocities of sideband photons using PCFs. Cui *et al.*[8] experimentally demonstrated that besides the intrinsic oscillation of the phase matching func-

*Supported by the State Key Program for Basic Research of China under Grant No. 2012CB921802, the National Natural Science Foundation of China under Grant Nos. 91321312, 91121001, 11321063, 11174121, and 61475099, and the Project Funded by the Priority Academic Program Development of Jiangsu Higher Education Institutions (PAPD), and the Program for New Century Excellent Talents in University (NCET), and a Foundation for the Author of National Excellent Doctoral Dissertation of People's Republic of China (FANEDD)
†E-mail: pingxu520@nju.edu.cn

tion, the chirp of the pulsed pump and high-order dispersion can also effectively influence the frequency correlation of photon pairs. Unlike the fiber-based SFWM schemes, the complete joint spectral intensity (JSI) of SWW can not be easily measured as the pump frequency lies in the center. Very recently, it has been demonstrated that the whole JSI can be measured by the classical stimulated process with a fast and reliable quality control procedure.[20] Hence in this paper, we analyze the spectral properties of entangled photon pairs generated in an SWW via SFWM. Our motivation for this work is to study the effects of dispersion, waveguide structure, pump pulse and two-photon absorption, which are relevant in the production of a wide range of spectral correlation, factorability and anticorrelation in the two-photon component of the state. The specific sources of integrated SWW play a significant role in quantum information processing applications. Furthermore, by employing the Schmidt number, the degree of frequency entanglement is studied and it shows a significant dependence on the factors mentioned above.

2 Theoretical Model

In the process of SFWM, two pump photons at frequency ω_{p1} and ω_{p2} are converted into a pair of energy-time-entangled signal and idler photons at frequency ω_s and ω_i, respectively, moderated by a third-order nonlinear optical material. The special case, in which $\omega_{p1} = \omega_{p2}$, is interesting because FWM can be initiated with a single pump beam. This degenerate case is often useful for SWW. Although the vectorial four-photon scattering are also allowed in the birefringent SWW, we focus on the case in which a single pump pulse with a central wavelength of 1.55 μm polarized along one of the principal axes of a birefringent SWW, i.e. the scalar case, where the three waves are copolarized in either TM or TE mode inside a waveguide. The relationship between ω_p, ω_s and ω_i is $2\omega_p = \omega_s + \omega_i$. SFWM inside the SWW can be phenomenologically described using the interaction Hamiltonian

$$H_I = 4\epsilon_0\chi^{(3)} \int \mathrm{d}\vec{r} E_p^{(+)} E_p^{(+)} \hat{E}_s^{(-)} \hat{E}_i^{(-)} + \mathrm{h.c.}\,,$$

where pump pulse propagating along the waveguide remains classical, and can be expressed as[8]

$$E_p^{(+)} = A\,\mathrm{e}^{-\mathrm{i}\gamma P_p z} \int \mathrm{d}\omega_p \exp\Big[-\frac{(\omega_p-\omega_{\mathrm{pc}})^2}{2\sigma_p^2} - \mathrm{i}\phi(\omega_p)\Big] \times \mathrm{e}^{\mathrm{i}(\beta_p z-\omega_p t)}, \quad (1)$$

where ω_{pc} and σ_p are the central frequency and bandwidth of the pump beam respectively. γ represents the nonlinear coefficient of the SWW and P_p is the peak power. $\phi(\omega_p)$ is the frequency-dependent spectral phase due to the effects of chromatic dispersion and Kerr nonlinearity when the pump propagates in the SWW. After the Taylor expansion of $\phi(\omega_p)$ and omitting the high-order terms $\phi(\omega_p) = \phi_0 + \phi_1(\omega_p - \omega_{\mathrm{pc}}) + \phi_2(\omega_p - \omega_{\mathrm{pc}})^2/2$. The expression of the pump pulse can be simplified as

$$E_p^{(+)} = A\,\mathrm{e}^{-\mathrm{i}\gamma P_p z} \int \mathrm{d}\omega_p \exp\Big[-\frac{(\omega_p-\omega_{\mathrm{pc}})^2}{2\sigma_p^2}(1+\mathrm{i}C_p)\Big]\,\mathrm{e}^{\mathrm{i}(\beta_p z-\omega_p t)}, \quad (2)$$

where $C_p = \sigma_p^2\phi_2$ is the linear chirp of the pump. The peak power and pulse duration of the chirp pulse can be expressed as $P_p \propto A^2\omega_p^2/\sqrt{1+C_p^2}$ and $T_p = 2\sqrt{\ln 2}\sqrt{1+C_p^2}/\sigma_p$ respectively. $C_p = 0$ corresponds to the fourier transformed limited pulse, i.e. a broadband pulse should be short in time. In the low-gain regime, it is reasonable to quantize the signal and idler fields, which are both at the single-photon level:

$$E_j^{(-)} = \int \mathrm{d}\omega_j \sqrt{\frac{\hbar\omega_j}{2\varepsilon_0 V_q}} \frac{a^{(+)}(\omega_j)}{n(\omega_j)}\,\mathrm{e}^{-\mathrm{i}(\beta_j z-\omega_j t)}, \quad (3)$$

with $j = s$ or i. $a^{(+)}(\omega_j)$ is the creation operator of the vacuum field at ω_j. Hence the interaction Hamilton can be written as

$$H_I = \frac{\gamma P_p L\sqrt{1+C_p^2}}{\sigma_p^2} \int \mathrm{d}\omega_p \mathrm{d}\omega_s \mathrm{d}\omega_i \exp[-\mathrm{i}(2\omega_p-\omega_s-\omega_i)t] \times \exp\Big[-\frac{(\omega_s+\omega_i-2\omega_{\mathrm{pc}})^2}{4\sigma_p^2}(1+\mathrm{i}C_p)\Big]\mathrm{sinc}\Big(\frac{\Delta kL}{2}\Big), \quad (4)$$

where Δk denotes the wave vector mismatch. It can be expressed as

$$\Delta k = \Delta k_M + \Delta k_W + 2\gamma P_p\,. \quad (5)$$

Δk_M and Δk_W represent the mismatch occurring as a result of material dispersion and waveguide dispersion respectively. In the case of a single-mode waveguide, $\Delta k_W = 0$, since the change in the material index due to waveguiding is nearly the same for all waves. The third term is the nonlinear part resulting from the self-phase modulation introduced by the pump wave. Here we assume that the pump powers are low such that self-phase modulation are negligible and thus the phase-matching conditions do not depend on the power. Moreover, for photon-pair generation, the pump power should be kept low enough that $\gamma P_p L \leq 0.2$ to prevent stimulated scattering.[11] As the signal and idler are located symmetrically around the pump frequency, the phase mismatch due to material dispersion depends only on even-order dispersion parameters.[13,21] Therefore $\Delta k = 2\beta(\omega_p) - \beta(\omega_s) - \beta(\omega_i)$. Using the Taylor expansion of $\beta(\omega_p)$, $\beta(\omega_s)$ and $\beta(\omega_i)$ at the central frequency, respectively, we obtain

$$\Delta k = \tau_s(\omega_s-\omega_{s0})^2 + \tau_i(\omega_i-\omega_{i0})^2 + \frac{\beta_{\mathrm{pc}}^{(2)}}{2}(\omega_s-\omega_{s0})(\omega_i-\omega_{i0})\,, \quad (6)$$

where $\tau_{s(i)} = \beta_{\mathrm{pc}}^{(2)}/4 - \beta_{s(i)0}^{(2)}/2$ and $\beta_j^{(2)} = \mathrm{d}^2\beta/\mathrm{d}\omega^2|_{\omega_j}$

$(j = \mathrm{pc}, s0, i0)$ is the second-order dispersion parameter. The two-photon quantum state $|\Psi\rangle$ at the output of the nonlinear crystal can be expressed as $|\Psi\rangle = |\mathrm{vac}\rangle - i/\hbar \int \mathrm{d}t H_I(t)|\mathrm{vac}\rangle$. The joint spectral amplitude evaluated from first-order perturbation theory can be written as

$$\psi(\Omega_s, \Omega_i) \propto \exp\Big[-\frac{\Omega_+^2(1+\mathrm{i}C_p)}{4\sigma_p^2}\Big]\mathrm{sinc}\Big[\frac{\beta_{\mathrm{pc}}^{(2)} L\Omega_-^2}{8}\Big], \quad (7)$$

where $\Omega_\pm = \Omega_s \pm \Omega_i$ and $\Omega_{s(i)} = \omega_{s(i)} - \omega_{s0(i0)}$.

The most developed approach to quantitative analysis bipartite entanglement is based on using coherent modes decomposition, i.e. Schmidt decomposition, $|\Psi\rangle_{AB} = \sum_n \sqrt{\lambda_n}|\phi_n\rangle_A|\varphi_n\rangle_B$, where $|\phi_n\rangle_A$, $|\varphi_n\rangle_B$ are the Schmidt modes defined by eigenvectors of the reduced density matrices for the signal and idler photons, respectively, and $\sqrt{\lambda_n}$ are the corresponding eigenvalues, with λ_n represents the probability of finding the entangled state in the n-th entangled Schmidt mode $|\phi_n\rangle_A|\varphi_n\rangle_B$. Once the Schmidt coefficients are obtained, one can obtain $K = 1/\sum_n \lambda_n^2$, which can be interpreted as a measure of the effective dimensionality of the system.

3 Spectral Properties of Correlated Photon Pairs

We consider the strip waveguide structure fabricated on an SOI wafer with a Si top layer on a 3 μm SiO_2 layer. The SWW was 460-nm wide, 200-nm thick, which is widely used in experiments.[14–16] We calculated the effective refractive index by using the finite-element method (commercial software COMSOL simulation).[22] Figure 1 shows the effective index of refraction of the TM and TE modes as a function of wavelength for the waveguide structure. The group index n_g, defined as $n_g = \beta^{(1)}c$, of the TM mode is shown in the inset of Fig. 1. n_g can also be engineered by controlling the configuration of the chip.[13,22] Without loss of generality, we focus on the discussion of TM mode in the following discussion. The second-order dispersion parameter of TM mode at 1550 nm, which can be differentiated numerically from $\beta^{(1)}$ using a spline-fit procedure, is 0.21 ps^2/cm.

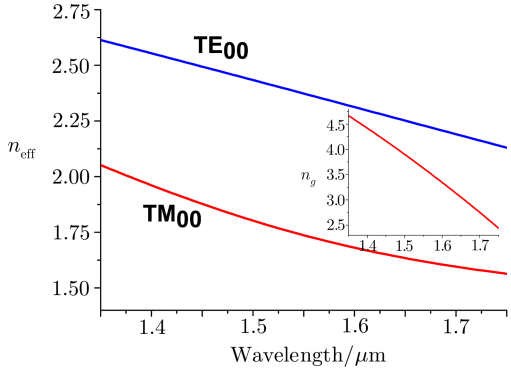

Fig. 1 Plots of computed effective index of refraction of TE_{00} and TM_{00} modes as a function of wavelength. Inset, the group index of TM_{00} mode.

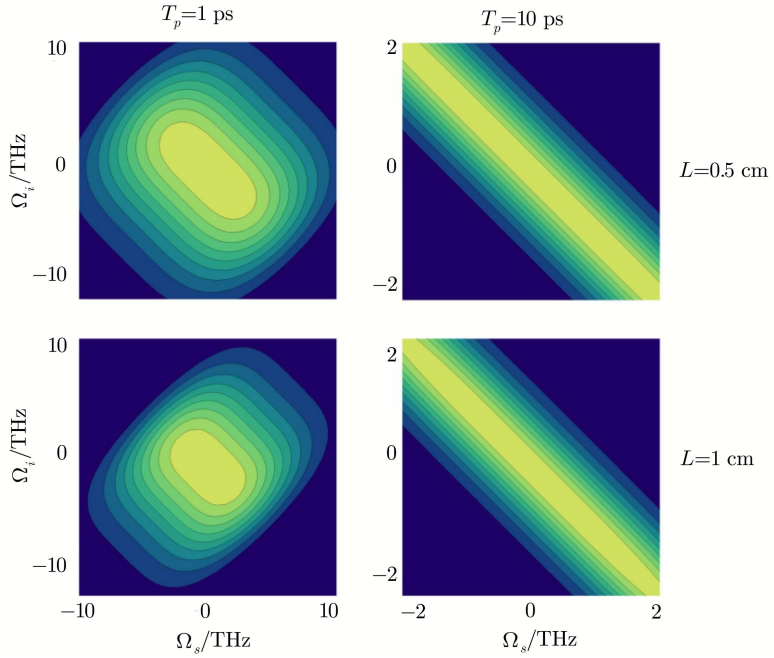

Fig. 2 The joint spectra for different pump bandwidths and waveguide lengths as a function of signal and idler detuning frequency.

In Fig. 2, we plot the contour map of joint spectra for different pump durations ($T_p = 1$ ps and 20 ps) and waveguide lengths ($L = 0.5$ cm and 1 cm) as a function of signal and idler detuning frequency with $C_p = 0$. It is clear that the frequency correlation can be negatively or positively correlated by detuning the waveguide lengths or the pump pulse duration. A joint spectral amplitude with a circular form implies a decorrelated state. One can achieve spectrally decorrelated joint spectral amplitude distributions by a careful choice of the waveguide lengths and pump

bandwidth. Although the phase-matching function is a sinc function with significant amplitude far from the central peak, the tails of the sinc function can be spectrally filtered out by using an arrayed waveguide grating.

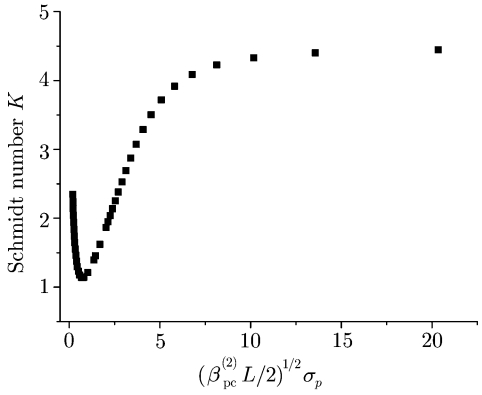

Fig. 3 The Schmidt number K, which quantifies the degree of entanglement, changes with the parameter $\sqrt{\beta_{\rm pc}^2 L/2}\sigma_p$ for $C_p = 0$.

By the numerical tool for calculating the Schmidt decomposition in systems with continuous degrees of freedom, the Schmidt numbers K are calculated and plotted in Fig. 3. We note that the Schmidt numbers are uniquely determined by the parameter $\sqrt{\beta_{\rm pc}^{(2)}L/2}\sigma_p$ despite the actual dimensions of L and ω_p. The demarcation point is $\sqrt{\beta_{\rm pc}^{(2)}L/2}\sigma_p = 0.73$ with $K = 1.14$, which corresponds to minimally frequency entangled state. For $\sqrt{\beta_{\rm pc}^{(2)}L/2}\sigma_p \gg 0.73$ (frequency positively correlated states) or $\sqrt{\beta_{\rm pc}^{(2)}L/2}\sigma_p \ll 0.73$ (frequency anti-correlated states), high degree of frequency entanglement can be achieved, which is more robust to the presence of noise and other deleterious environmental effects.

4 Influence of Pump Chirp on the Two-Photon State

The information pertaining to the linear chirp of the pump in the two-photon state, as can be seen from Eq. (7), is contained in the phase term. The sinc function that appears in Eq. (7) can be simplified by applying the Gaussian approximation, which retains the main features of the two-photon state.[23] We take $\mathrm{sinc}[bx^2] \approx \exp[-\alpha b x^2]$ with $\alpha = 0.725$, so that both functions coincide at the $1/e^2$ intensity. In this case, the temporal description of the two-photon state can be obtained as the two-dimensional Fourier transform of $\psi(\Omega_s, \Omega_i)$. The resulting expression is as follows

$$\psi(t_s, t_i) \propto \exp[A(t_s^2 + t_i^2) + 2Bt_s t_i]\,, \tag{8}$$

with

$$A = \frac{-2C_p + \mathrm{i}(2 + L\beta_{\rm pc}^{(2)}\alpha\sigma_p^2)}{4(-\mathrm{i} + C_p)L\beta_{\rm pc}^{(2)}\alpha}\,, \tag{9}$$

$$B = \frac{2C_p + \mathrm{i}(-2 + L\beta_{\rm pc}^{(2)}\alpha\sigma_p^2)}{4(-\mathrm{i} + C_p)L\beta_{\rm pc}^{(2)}\alpha}\,. \tag{10}$$

It is noted that the pump chirp has no effect on the JSI, but can influence the joint temporal intensity (JTI) obviously. In Fig. 4, we show the influence of pump chirp, presenting as an example the case of $T = 0.5$ ps and $L = 1$ cm. In this case we found that the frequency of a photon pair is positively correlated (see Fig. 4(a)), resulting from that the bandwidth of the phase-matching function is much narrower than that of the pump pulse. Also, when depicting the temporal correlation for $C_p = 0$, which corresponds to the Fourier transform of the pump pulse function and phase-matching function respectively, as shown in Eq. (8), we found that the bandwidth of $t_s + t_i$ is narrower than that of $t_s - t_i$, so the temporal correlation is anticorrelated. However, as can be seen from Fig. 4(c), the temporal correlation is positively correlated for $C_p = 6$, representing the pump chirp makes the two-photon wavepackets not Fourier transform-limited, i.e., frequency-correlation does not necessarily imply time-anticorrelation. The physical origin is that the phase term due to pump chirp acts as an elongation of the JTI along the direction given by $t_s + t_i$, resulting in the bandwidth of $t_s + t_i$ broader than that of $t_s - t_i$.

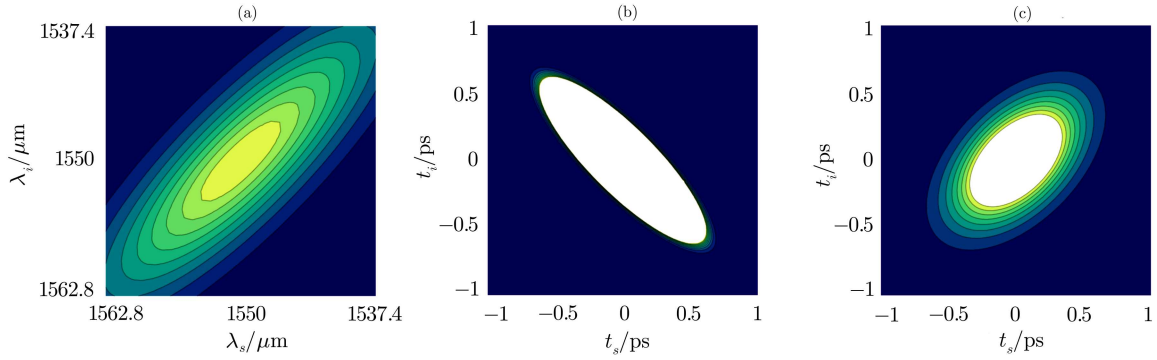

Fig. 4 Influence of chirp on the temporal properties of the two-photon state: (a) Contour map of joint spectral intensity; (b) the corresponding contours of joint temporal intensity for $C_p = 0$; and (c) contours of joint temporal intensity for $C_p = 6$.

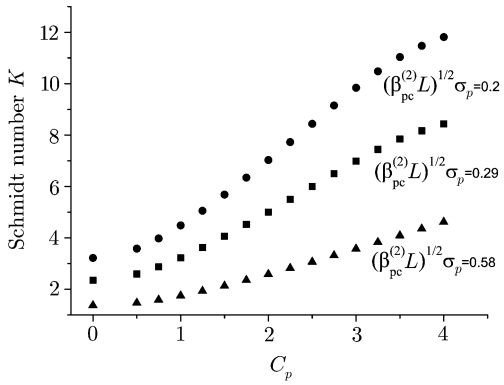

Fig. 5 The behavior of the Schmidt number as a function of the pump chirp parameter for three different values of $\sqrt{\beta_{\rm pc}^{(2)}L}\sigma_p$.

To learn how the linear chirp of the pump influences the frequency entanglement, we plot in Fig. 5 the Schmidt number as a function of C_p for three different values of $\sqrt{\beta_{\rm pc}^{(2)}L}\sigma_p$. It is evident that the Schmidt number increases with increasingly larger values of C_p. The physical origin is that the contribution of pump chirp to entanglement in the spectral domain is in the form of phase entanglement.[23] As can be seen from Eq. (7), the phase term associated with a chirped pump can not be factored into signal and idler factors, the $\Omega_s\Omega_i$ does exist and always contribute to entanglement. Hence, the pump chirp can be used as an effective tool to control the degree of frequency entanglement in SWWs. The photon source with high K is applicable for protocols using frequency entanglement such as a multi-user entangled photon distribution.[24]

5 Influence of the Nonlinear Losses on the Two-Photon State

In the presence of nonlinear losses, for example two-photon absorption (TPA), the two-photon quantum state can be derived iteratively using the standard Dyson's perturbation expansion from quantum theory of scattering.[9] Therefore the joint spectral amplitude can be written as[25]

$$\psi(\Omega_s,\Omega_i)\propto\exp\Big[-\frac{\Omega_+^2}{4\sigma_p^2}\Big]\frac{\sinh[gL]}{gL}\,, \tag{11}$$

where g is the parametric gain term and can be defined as

$$g=\sqrt{\Big(\frac{\phi}{L}\Big)^2-\Big(\frac{\beta_{\rm pc}^{(2)}\Omega_-^2}{8}+\frac{\phi}{L}\Big)^2}\,. \tag{12}$$

ϕ is the nonlinear phase shift and can be expressed as[26]

$$\phi=\frac{k_0n_2}{\beta_{\rm TPA}}\ln[1+\beta_{\rm TPA}I_0L_{\rm eff}]\,, \tag{13}$$

where $L_{\rm eff}=(1-{\rm e}^{-\alpha_l}/\alpha_l)$ is the effective length for a waveguide of length L in the presence of propagation loss α_l, $k_0=2\pi/\lambda$, n_2 is the Kerr coefficient, $\beta_{\rm TPA}$ is the TPA coefficient, I_0 accounts for the input peak intensity. We neglect both the effects of free-carrier absorption and free-carrier dispersion in the limit of the peak intensity of the pump pulse is not too high. It is reasonable when the input peak intensity I_0 satisfies the condition $I\ll 3h\nu_0/(\sigma T_p)$, where $\sigma=1.45\times10^{-21}$ m^2 is the free-carrier absorption cross section for $\lambda=1.55$ μm.[24] For example, $I_0\ll 27$ GW/cm^2 for $T_p=1$ ps. At the 1.55 μm wavelength, $n_2\approx 6\times10^{-18}$ m^2/W, $\beta_{\rm TPA}\approx 5\times10^{-12}$ m/W. In this case, we focus on the SOI waveguide with $\alpha_l=1$ dB/cm.

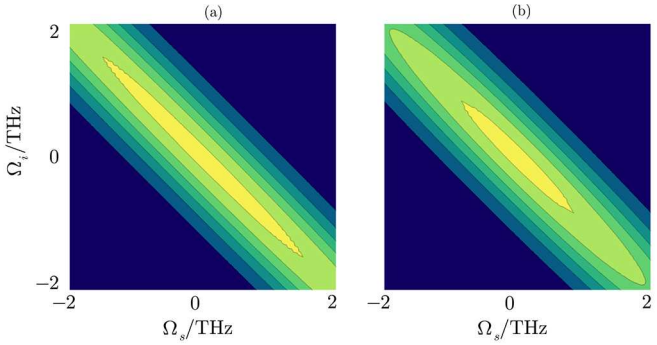

Fig. 6 Influence of input peak intensity on the spectral properties of the two-photon state with the pulse width $T_p=10$ ps, waveguide length $L=0.5$ cm.

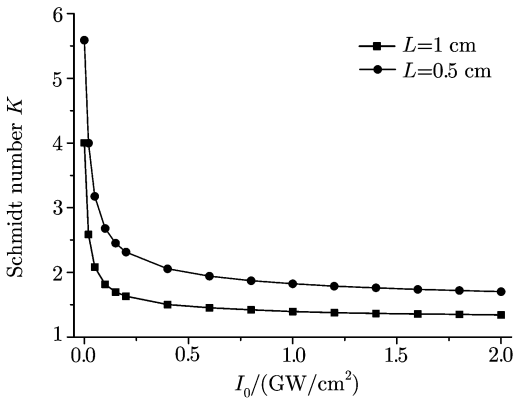

Fig. 7 Schmidt number is given as a function of I_0 when $T_p=10$ ps for two different waveguide lengths.

In Figs. 6(a) and 6(b), by choosing the pump peak intensity I_0 ($I_0=0.5$ GW/cm^2 for Fig. 6(a), $I_0=1$ GW/cm^2 for Fig. 6(b)), namely the nonlinear phase shift, we find that I_0 can brings different characters to the spectral correlation. In Fig. 7, by evaluating the Schmidt number as a function of I_0 for two different waveguide lengths, we find the Schmidt number always decreases as I_0 enlarging. Meanwhile, the nonlinear losses also impose an intrinsic limit on heralded single photon sources.[25]

6 Conclusion

In conclusion, we have analyzed the spectral properties of photon pairs generated in telecom C-band inside a dispersion-engineered SWW with well-defined guided modes. The joint spectral shape of the produced two-photon state is presented, which depends mainly on the waveguide length, pump duration, two relatively easy experimental parameters to control. The parameter $\sqrt{\beta_{\rm pc}^{(2)}L}\sigma_p$ uniquely determines the wavefunction, spectral correlation and the Schmidt number of such single modes

photon pairs. Additionally, we find that pump chirp which is due to the effect of chromatic dispersion and Kerr nonlinearity in a dispersive waveguide can constitute an effective tool for the control of the degree of frequency entanglement. For the pump peak intensity is not too high, the induced nonlinear losses of the waveguide can also influence the biphoton spectral features obviously and impose an intrinsic limit on the achievement of high degree of frequency entanglement. In view of the results obtained here, it could be possible to devise SWWs that turn out to be beneficial for applications in the area of chip-scale quantum information processing.

References

[1] S.L. Braunstein and P. van Loock, Rev. Mod. Phys. **77** (2005) 513.

[2] S.W. Du, J.M. Wen, M.H. Rubin, and G.Y. Yin, Phys. Rev. Lett. **98** (2007) 053601.

[3] S.W. Du, J.M. Wen, and M.H. Rubin, J. Opt. Soc. Am. B **25** (2008) C99.

[4] G.P. Agrawal, *Nonlinear Fiber Optics*, 3rd ed, Academic Press, New York (2001).

[5] J.M. Wen, S.W. Du, and M.H. Rubin, Phys. Rev. A **75** (2007) 033809.

[6] X. Li, J. Chen, P. Voss, J. Sharping, and P. Kumar, Opt. Express **12** (2004) 3737.

[7] L. Cui, X.Y. Li, and N.B. Zhao, Phys. Rev. A **85** (2012) 023825.

[8] L. Cui, X.Y. Li, and N.B. Zhao, New. J. Phys. **14** (2012) 123001.

[9] E. Brainis, Phys. Rev. A **79** (2009) 023840.

[10] J. Suo, S. Dong, W. Zhang, Y.D. Huang, and J.D. Peng, Opt. Express **23** (2015) 3985.

[11] Q. Lin, Oskar J. Painter, and G.P. Agrawal, Opt. Express **15** (2007) 16604.

[12] Q. Lin and Govind P. Agrawal, Opt. Lett. **31** (2006) 3140.

[13] Q. Lin, J. Zhang, P.M. Fauchet, and G.P. Agrawal, Opt. Express **14** (2006) 4786.

[14] J.W. Silverstone, D. Bonneau, K. Ohira, *et al.*, Nat. Photon. **8** (2014) 104.

[15] H. Takesue, Y. Tokura, H. Fukuda, T. Tsuchizawa, T. Watanabe, K. Yamada, and S. Itabashi, Appl. Phys. Lett. **91** (2007) 201108.

[16] K. Harada, H. Takesue, H. Fukuda, T. Tsuchizawa, T. Watanabe, K. Yamada, Y. Tokura, and S. Itabashi, Opt. Express **16** (2008) 20368.

[17] Y. Guo, W. Zhang, N. Lv, Q. Zhou, Y. Huang, and J. Peng, Opt. Express **22** (2014) 2620.

[18] W.P. Grice, A.B. U'Ren, and I.A. Walmsley, Phys. Rev. A **64** (2001) 063815.

[19] K. Garay-Palmett. H.J. McGuinness, O. Cohen, *et al.*, Opt. Express **15** (2007) 14870.

[20] M. Liscidini and J.E. Sipe, Phys. Rev. Lett. **111** (2013) 193602.

[21] M.E. Marhic, N. Kagi, T.K. Chang, and L. G. Kazovsky, Opt. Lett. **21** (1996) 573.

[22] R.M. Osgood, Jr., N.C. Panoiu, J.I. Dadap, *et al.*, Adv. Opt. Photonics **1** (2009) 162.

[23] K.W. Chan, J.P. Torres, and J.H. Elberly, Phys. Rev. A **75** (2007) 050101(R).

[24] I. Herbauts, B. Blauensteiner, A. Poppe, T. Jennewein, and H. Hubel, Opt. Express **21** (2013) 29013.

[25] C. Husko, A. Clark, M. Collins, A. Rossi, S. Combrie, G. Lehoucq, I. Rey, T. Krauss, C. Xiong, and B. Eggleton, Sci. Rep. **3** (2013) 3087.

[26] L.H. Yin and G.P. Agrawal, Opt. Lett. **21** (2007) 2031.